

# Interactions of tricyclic antipsychotic and antidepressant medications with a novel binding site in GABA<sub>A</sub> receptors

Konstantina Bampali (1), Filip Koniuszewski (1), Luca Silva (1), Sabah Rehman (2), Florian D. Vogel (1), Thomas Seidel (3), Florian Zirpel (1), Arthur Garon (3), Thierry Langer (3), Matthäus Willeit (4), Margot Ernst\* (1)

(1) Department of Pathobiology of the Nervous System, Center for Brain Research, Medical University Vienna, Spitalgasse 4, 1090 Vienna, Austria

(2) Department of Molecular Neurosciences, Center for Brain Research, Medical University of Vienna, Spitalgasse 4, 1090 Vienna, Austria

(3) Department of Pharmaceutical Sciences, Division of Pharmaceutical Chemistry, University of Vienna, Althanstraße 14, 1090 Vienna, Austria

(4) Department of Psychiatry and Psychotherapy, Medical University of Vienna, Währinger Gürtel 18-20, 1090, Vienna, Austria

\*Corresponding author: [margot.ernst@meduniwien.ac.at](mailto:margot.ernst@meduniwien.ac.at), phone number: +43 1 40160 34065

## Abstract

**Background and Purpose:** Many psychotherapeutic drugs including clozapine have a polypharmacological profile and act on GABA<sub>A</sub> receptors, where subtype-specific information is often lacking. Patients with schizophrenia show alterations in function, structure and molecular composition of the hippocampus, and a recent study demonstrated aberrant levels of hippocampal  $\alpha 5$  subunit containing GABA<sub>A</sub> receptors.

**Experimental Approach:** Functional studies of GABA modulatory effects by antipsychotic and antidepressant medications were performed in several GABA<sub>A</sub> receptor subtypes by two-electrode voltage-clamp electrophysiology using *Xenopus laevis* oocytes. Computational structural analysis was employed to design mutated constructs of the  $\alpha 5$  subunit, probing a novel binding site. Computational ligand analysis complemented the functional and mutational data.

**Key Results:** We show that the antipsychotic drugs clozapine and chlorpromazine have negative modulatory effects on multiple GABA<sub>A</sub> receptor subtypes, including  $\alpha 5$ -containing. On the latter we show negative modulatory effects for five additional antipsychotic and antidepressant drugs. Based on a chlorpromazine binding site observed in a GABA-gated bacterial homologue, we identified a novel site in  $\alpha 5$  GABA<sub>A</sub> receptor subunits.

**Conclusion and Implications:** Our findings support previous studies suggesting a link between some of the therapeutic effects of clozapine and its negative modulatory action on certain GABA<sub>A</sub> receptor subtypes. The novel site we describe in this study is a new potential target for optimizing antipsychotic medications with beneficial polypharmacology.

## Introduction

Hippocampal dysfunction has long been considered to contribute to the pathophysiology of schizophrenia<sup>1-3</sup>. Post-mortem studies in the brains of patients with schizophrenia suggest that expression of GABA<sub>A</sub> receptors in the prefrontal cortex and hippocampus is altered in a subtype-selective manner<sup>4</sup>. The  $\alpha 5$  GABA<sub>A</sub> receptor subunit, which is characterized by its relatively limited distribution and high abundance in the hippocampus, has thus been in the focus of clinical and preclinical schizophrenia research<sup>5,6</sup>. A recent positron emission tomography (PET) study using [<sup>11</sup>C]Ro15-4513, a radioligand binding with high affinity to  $\alpha 5$ -containing GABA<sub>A</sub> receptor subtypes, found evidence for aberrant receptor levels in the hippocampus of patients with schizophrenia<sup>5</sup>. Moreover, the study demonstrated a direct relationship between the expression of schizophrenia symptoms and hippocampal binding of [<sup>11</sup>C]Ro15-4513. [<sup>11</sup>C]Ro15-4513 binds at the benzodiazepine site of GABA<sub>A</sub> receptors in which the  $\alpha 5$  subunit is localized next to a  $\gamma 2$  subunit<sup>7</sup>. The quest for  $\alpha 5$ -containing subtype-preferring ligands, with emphasis on benzodiazepine analogues, has provided a number of compounds widely used in research<sup>8-10</sup>. These molecules exert allosteric modulatory effects that can range from GABA-induced current enhancement or reduction to silent but competitive binding, effects which are nowadays termed as positive, negative, and silent allosteric modulation (or PAM/NAM/SAM), respectively<sup>11</sup>. Historical terms such as benzodiazepine receptor agonism, antagonism and inverse agonism are also in frequent use<sup>11</sup>. Based on genetic and pharmacological studies, drugs which target  $\alpha 5$ -containing GABA<sub>A</sub> receptors have been under investigation as cognitive enhancers for considerable time<sup>6</sup>. For instance, deletion or reduction in the amount of  $\alpha 5$ -containing GABA<sub>A</sub> receptors was associated with enhanced learning<sup>6</sup>. Negative modulation of  $\alpha 5$ -containing GABA<sub>A</sub> receptors has also been shown to promote hippocampal gamma oscillations, long-term potentiation, and learning, as well as have antidepressant effects associated with restored synaptic strength in the form of increased glutamatergic excitatory activity<sup>6,12,13</sup>. Among the most recent developments was a clinical trial examining basmisanil, a compound exerting NAM effects at  $\alpha 5$ -containing GABA<sub>A</sub> receptors, as an add-on treatment for antipsychotic therapy aiming to alleviate cognitive impairment of patients with schizophrenia (<https://clinicaltrials.gov/ct2/show/NCT02953639>).

Not only GABA<sub>A</sub> receptor targeting drugs such as benzodiazepines or sedative general anesthetics elicit effects at these receptors by allosteric interaction sites, but a wide range of small molecules have been identified as GABA<sub>A</sub> receptor modulators, including multiple antipsychotic and antidepressant medications not intentionally targeting these receptors<sup>14,15</sup>. One of those is clozapine (CLZ), a tetracyclic compound displaying relatively weak dopamine receptor antagonism. However, it shows outstanding antipsychotic efficacy and ameliorates negative and cognitive symptoms of schizophrenia without inducing unwanted extrapyramidal side effects<sup>16,17</sup>. On the other hand chlorpromazine's (CPZ) antipsychotic effects were mainly attributed to blockade of dopamine receptors and has received only minor attention in terms of its effects on GABA<sub>A</sub> receptors<sup>18-21</sup>. There is broad consensus that CLZ can reduce GABA elicited effects by direct interactions with GABA<sub>A</sub> receptors, however, the mechanism remains unclear and the binding sites were never identified<sup>22-25</sup>. In the 80's and 90's, the interactions of several antipsychotics with GABA<sub>A</sub> receptors have been considered serious candidates for eliciting part of the therapeutic effects but were never studied in  $\alpha 5$ -containing receptors<sup>14,15,24,26,27</sup>.

In this work, we bridge this gap and examine the functional effects of CLZ and six compounds with overlapping and distinctive pharmacophore features in recombinantly expressed GABA<sub>A</sub> receptors, including  $\alpha 5$ -containing receptors. We demonstrate allosteric negative modulation across a range of efficacy from weak to strong. To further elucidate the molecular substrate of the observed NAM effects, we investigate a novel intrasubunit binding site in the extracellular domain of the  $\alpha 5$  subunit, which has been described as a CPZ site in a homologous GABA-gated pentameric ligand-gated ion channel (pLGIC)<sup>28</sup>. This finding opens new avenues for the rational development of drugs that target  $\alpha 5$ -containing GABA<sub>A</sub> receptors, whose established importance in cognitive functions in psychiatric and affective disorders prompt their serious consideration as a therapeutic target.

## Results

### Negative modulatory profile of CLZ on different GABA<sub>A</sub> receptor subtypes

First, we examined CLZ effects on recombinantly expressed GABA<sub>A</sub> receptors. We performed functional testing of the drugs' effects in the most expressed receptor subunits in the central nervous system<sup>29</sup>, as well as the subtypes discussed in the literature as candidate targets for alleviating some schizophrenia symptoms, namely  $\alpha 2$  and  $\alpha 5$ -subunit containing GABA<sub>A</sub> receptors<sup>6</sup>. Specifically, we studied CLZ effects on nine assemblies ( $\alpha 1\beta 2$ ,  $\alpha 1\beta 3$ ,  $\alpha 1\beta 3\gamma 2$ ,  $\alpha 2\beta 3$ ,  $\alpha 2\beta 3\gamma 1$ ,  $\alpha 2\beta 3\gamma 2$ ,  $\alpha 5\beta 3\gamma 2$ ,  $\alpha 5\beta 2\gamma 2$  and  $\beta 2\gamma 2$ ) that have not been investigated at all in previous studies (Figure 1). In earlier experiments where a different subtype panel was investigated, inhibitory as well as biphasic modulation of radioligand binding was observed<sup>22</sup>, prompting us to use a lower GABA concentration (EC<sub>5-10</sub>) for the functional assessment. Only negative modulation was seen in the tested range CLZ 1- 100 $\mu$ M, no PAM or biphasic effects (Supplementary Fig. S1). The effects we observed by co-application of 100 $\mu$ M CLZ with GABA EC<sub>5-10</sub> are summarized in Figure 1a. In five subunit combinations, the NAM effect approached its maximum effect at around 100 $\mu$ M, but the extent of inhibition varied (Figure 1c, Supplementary Figure S1). Inhibition in the tested  $\alpha 1$ -containing assemblies was less pronounced compared to  $\alpha 2$ -containing assemblies. The  $\alpha 5\beta 3\gamma 2$  combination displayed a similar effect to  $\alpha 2\beta 3\gamma 2$ . Overall, the identity or absence of the gamma isoform appears to impact less on the degree of inhibition compared to the alpha isoform. Inhibition remained incomplete (Supplementary Figure S1), supporting the proposed allosteric (NAM) mechanism of action. In the major receptor isoform<sup>29</sup> we successfully reproduced inhibitory effects on  $\alpha 1\beta 2\gamma 2$  receptors at 100 $\mu$ M CLZ (Figure 1a)<sup>30</sup>. Korpi *et al* also speculated that the efficacy of CLZ in  $\alpha 2$ -containing GABA<sub>A</sub> receptors would be higher than in  $\alpha 1$ , which can be confirmed by our results<sup>22</sup>. We also examined whether CLZ could inhibit neurosteroid activated currents. Neurosteroids, like THDOC, have been shown to directly activate GABA<sub>A</sub> receptors<sup>31</sup>. Here, CLZ does not inhibit THDOC-gated currents in  $\alpha 1\beta 3$  GABA<sub>A</sub> receptors (Figure 1b).

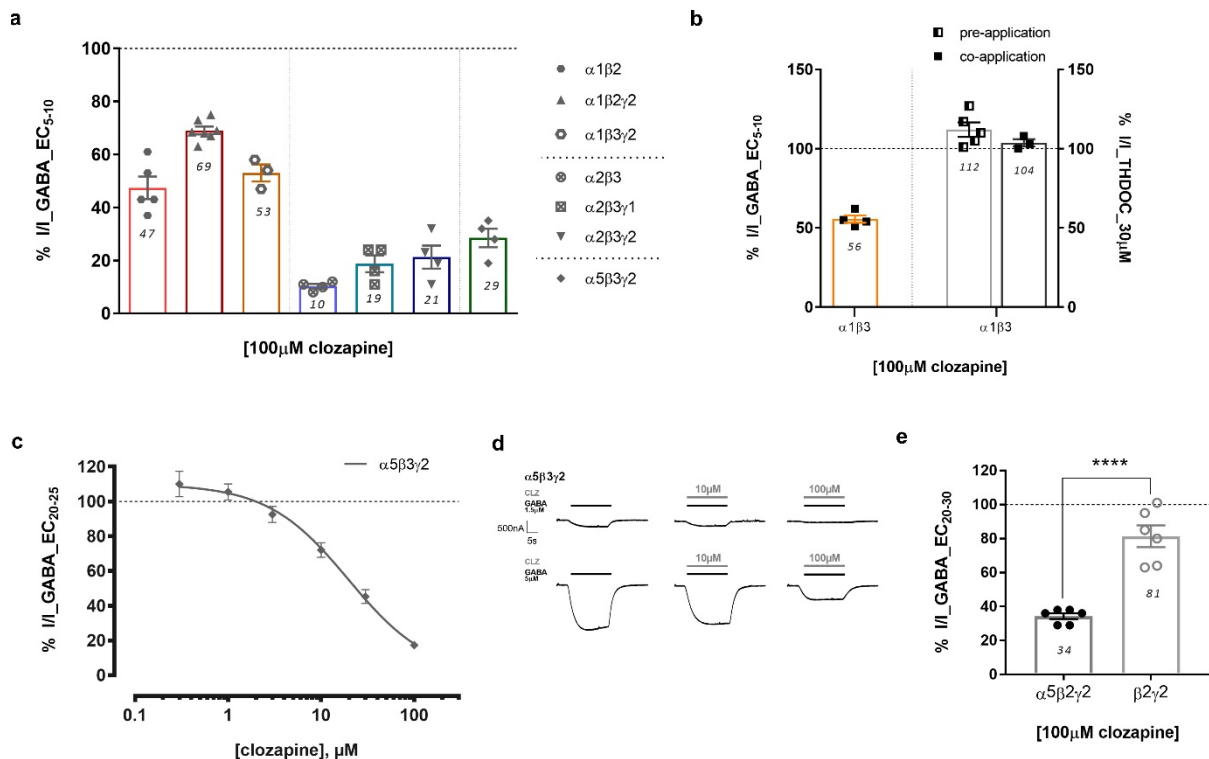


**Figure 1. Negative modulatory profile of CLZ on different GABA<sub>A</sub> receptor subtypes.** (a, b) Modulation of currents elicited by an EC<sub>5-10</sub> GABA concentration by 100 μM CLZ in α1β2, α1β2γ2, α1β3γ2, α2β3, α2β3γ1, α2β3γ2 and α5β3γ2 receptors (a), in α1β3 receptors (left y axis) (b) and by 30 μM concentration of the neurosteroid THDOC in α1β3 receptors (right y axis). Columns for each receptor subtype depict mean ± SEM and represent experiments from n = 3–7 oocytes from ≥2 batches. The dotted line is used to visualize the baseline (100%) of control current. (c) CLZ modulation of currents elicited by an EC<sub>20-25</sub> GABA concentration in α5β3γ2 receptors. Data were fitted to the Hill equation using non-linear regression (fixed bottom of 0 and slope of 1) and points are depicted as mean ± SEM. Each data point represents experiments from n = 4–7 oocytes from ≥2 batches. The dotted line is used to visualize the baseline (100%) of control current. (d) Representative traces from electrophysiological recordings of CLZ co-applied with two different concentrations of GABA in α5β3γ2 receptors; top traces corresponding to panel (a) and bottom traces to panel (c). (e) Modulation of currents elicited by an EC<sub>20-30</sub> GABA concentration by 100 μM CLZ in α5β2γ2 and β2γ2 receptors. Columns for each receptor subtype depict mean ± SEM and represent experiments from n = 6 oocytes from ≥2 batches. Statistically significant differences were determined by two-tailed students t-test, where p < 0.05; \*\*\*\*p < 0.0001. One sample t test was performed to determine statistical significance of each mean response from control current, where p < 0.05. Responses in both subtypes were found to be significantly different from control GABA current.

Due to the established role of α5 subunits in schizophrenia, we decided to test CLZ in α5-containing GABA<sub>A</sub> receptors in more detail. Here, we show that CLZ can dose-dependently inhibit α5β3γ2 receptors with an IC<sub>50</sub> of 19.7 μM, reaching a nearly maximum inhibition at the highest concentration (Figure 1c, d). Moreover, in an effort to assess the impact of the alpha subunit on the observed effects, we investigated CLZ responses in α5β2γ2 and in β2γ2 receptors and found the differences to be statistically significant (Figure 1e). Our results show that the removal of the α5 subunit from the receptor assembly eliminates a significant part of the effect (Figure 1e).

## A CPZ site in a bacterial GABA-gated pLGIC

CPZ was shown to bind to a site of the extracellular domain in a bacterial GABA-gated channel, namely ELIC<sup>28</sup>. The chemical similarity between CPZ and CLZ supports the idea of a common binding site in GABA<sub>A</sub> receptors or their homologues. The binding site that was observed to be occupied by CPZ in ELIC (Figure 2)<sup>28</sup> is formed by hydrophobic sidechains located on strands 2, 6 and 10 and capped by the backside of segment F (also called “loop F”), which provides both hydrophobic and polar interactions (see Figure 2a for the overall architecture of this site). CPZ interacts with the pocket mainly via van der Waals contacts of the tricyclic core, while the sidechain forms polar interactions with hydrophilic groups of loop F (Figure 2a)<sup>28</sup>.

In order to investigate whether CPZ and CLZ might use a homologous site in GABA<sub>A</sub> receptor subunits, we performed a series of experiments with CPZ. First, we established that it has a similar subtype profile as CLZ (Figure 2b). While CPZ reduced GABA-induced currents in α1β3γ2, α2β3 and α5β3γ2 receptors, it did not have any effect on β2γ2 receptors (Figure 2b). While removal of the α5 subunit strongly reduced the CLZ effect, it abolishes the CPZ effect completely (Figure 2b). Thus, the alpha subunit is necessary, and likely to either contain the CPZ binding site, or contribute to the binding site. We proceeded to examine the intrasubunit site (its localization is depicted in Figure 2c), which does not overlap with any of the known sites at ECD interfaces.

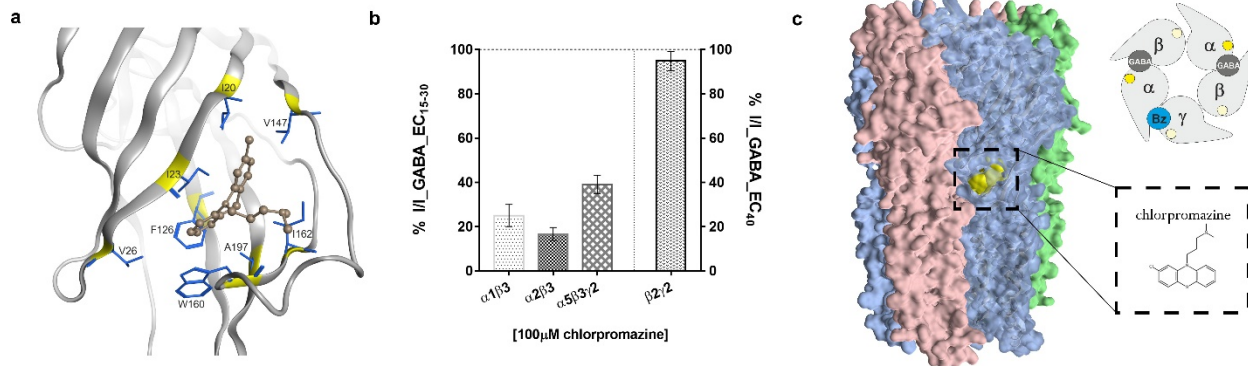


**Figure 2. Intra-subunit binding site occupied by CPZ in ELIC, and its corresponding localization in GABA<sub>A</sub> receptor subunits.** (a) ELIC-CPZ complex in 5LG3<sup>28</sup>, highlighting interacting residues. One chain of the protein is represented by grey ribbon. Interacting residues are additionally labeled and represented by licorice structures in blue. CPZ is represented in brown as a ball and stick structure. Hydrogen atoms are not displayed. (b) Modulation of currents elicited by an EC<sub>15-30</sub> GABA concentration by 100 μM CPZ in α1β3, α2β3 and α5β3γ2, (left y axis), as well as modulation of currents elicited by an EC<sub>40</sub> GABA concentration by 100 μM CPZ in β2γ2 receptors (right y axis). Columns for each receptor subtype depict mean ± SEM and represent experiments from n = 2–7 oocytes from ≥2 batches. One sample t test was performed to determine statistical significance of each mean response from control current in α5β3γ2 (n=7) and β2γ2 (n=5), where p<0.05. The response in α5β3γ2 was found to be significantly different from control GABA current, whereas in β2γ2 receptors was not significantly different. The dotted line is used to visualize the baseline (100%) of control current. (c) **Left:** A three dimensional representation of a heteropentameric GABA<sub>A</sub> receptor (PDB ID: 6A96) with CPZ docked into the corresponding ELIC binding site (CPZ in yellow space filling representation and its chemical structure in the figure inset). **Right:** Schematic of a commonly accepted subunit arrangement of a GABA<sub>A</sub> receptor indicating the location of the GABA binding site, the extracellular benzodiazepine binding site, as well as the novel binding site presented in this study. Solid yellow circles indicate the location of the novel intrasubunit binding site investigated in this study (faint yellow circles on beta and gamma subunits indicate the putative homologous sites).

We analyzed existing experimental structures to address the homology between the pocket seen in ELIC and GABA<sub>A</sub> receptor subunits. Recently published cryo-EM structures of α1βxγ2 (x = 1,2,3) receptors and α5β3 were analyzed (Figure 3, Supplementary Tables S1 and S2)<sup>32-35</sup>. The pocket localization observed in the bacterial superfamily members has been previously suggested to be compatible with homology models of GABA<sub>A</sub> receptors<sup>36</sup>, where it is located near the disulfide bridge in the packing core between the ECD inner and outer sheets (Figure 3).

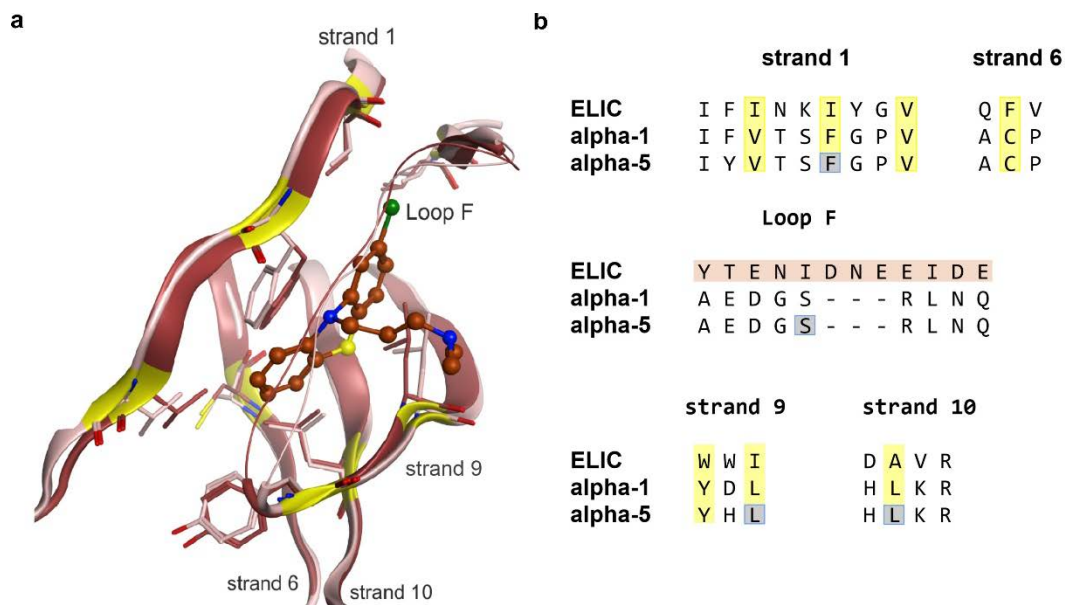


**Figure 3. Homology between the CPZ site in ELIC (5LG3) and the corresponding pocket in the  $\alpha$ 1 subunit of 6D6T and the  $\alpha$ 5 subunit of 6A96.** (a) 3D superposition of  $\alpha$ 1 (red) and  $\alpha$ 5 (pink) subunits of 6D6T and 6A96, respectively. Strands 1, 6 and 10 are highly conserved, and the hydrophobic amino acids forming the large deep portion of the pocket overlap closely. (b) Partial sequence alignment of the pocket forming protein segments of ELIC with the GABA<sub>A</sub> receptor  $\alpha$ 1 and  $\alpha$ 5 subunits. The hydrophobic pocket core positions are highlighted by yellow boxes and correspond with the yellow ribbon markings in panel (a). ELIC'S loop F segment highlighted in light pink, showing no structural correspondence between ELIC and  $\alpha$ 1,  $\alpha$ 5 subunits (see Supplementary Figure S2). The amino acids highlighted in grey boxes indicate sites chosen for mutational analysis (Figure 4a).

We found the region around this putative pocket to be quite conserved across all subunits (Figure 3, Supplementary Tables S1 and S2, Supplementary Figures S2 and S3). The hydrophobic pocket portion is very similar between ELIC and the GABA<sub>A</sub> receptor subunits from the atomic resolution structures mentioned above. Strands 1, 6 and 10 are highly conserved, and the hydrophobic amino acids forming the deep portion of the pocket overlap closely. Loop F in ELIC, however, shows no structural homology (Figure 3, Supplementary Figures S2 and S3). Additionally, the total pocket volume is quite different among subunits (Supplementary Table S1). While it is small in  $\beta$  and  $\gamma$  subunits, the  $\alpha$ 5 and  $\alpha$ 1 subunits have a candidate pocket of sufficient size to accommodate ligands of comparable size and shape to CPZ (Figure 3, Supplementary Table S1). Pocket volumes of the apo structures were slightly smaller than in ELIC (Supplementary Table S1), where mainly loop F position reduced the available cavity. We performed computational docking into the available alpha subunit structures to clarify if CPZ fits, and whether it assumes a pose similar to the one observed in the bacterial homologue. The structurally variable loop F was found to interfere weakly with the docking, but simulating flexibility with loop modelling resulted in CPZ docking results in  $\alpha$ 1 and  $\alpha$ 5 subunits with poses very similar to the original 5LG3 structure (Supplementary Figure S4).

### Mutational analysis of the putative binding site in the $\alpha$ 5 subunit impacts on compound effects

Next, we designed mutated  $\alpha$ 5 subunits. The four mutations were chosen based on pocket forming residues and their proximity to the ligand (Figure 4a, b). Moreover, one of those (Leu196, with the equivalent Ile in ELIC) was also mutated by Nys *et al* and was found to cause a significant reduction in the response of GABA and no significant change in EC50<sup>28</sup>. Bulky tryptophane residues were introduced into the four sites selected for mutational analysis in order to diminish the pocket volume (Figure 4a, b). To reduce the pocket volume even further we next selected two

of the tested residues, namely F53 and L222 for the generation of an  $\alpha 5$  double mutant (Figure 4c), which reduces the estimated volume of the binding site by 46%.

In our experiments, each  $\alpha 5$  subunit mutant was co-expressed individually with  $\beta 3$  and  $\gamma 2$ , forming an  $\alpha 5(\text{mut})\beta 3\gamma 2$  receptor. The GABA dose response curves of  $\alpha 5\text{F53W}\beta 3\gamma 2$ ,  $\alpha 5\text{L222W}\beta 3\gamma 2$  as well as  $\alpha 5\text{F53W};\text{L222W}\beta 3\gamma 2$  were matching the wild-type, in comparison to the other two that were right-shifted (Figure 4d). Diazepam effects ( $1\mu\text{M}$ ) were also examined in all mutated receptors and were found to be above  $\sim 200\%$  in wild-type and mutated receptors, which ensures the incorporation of the  $\gamma 2$  subunit (Figure 4e).

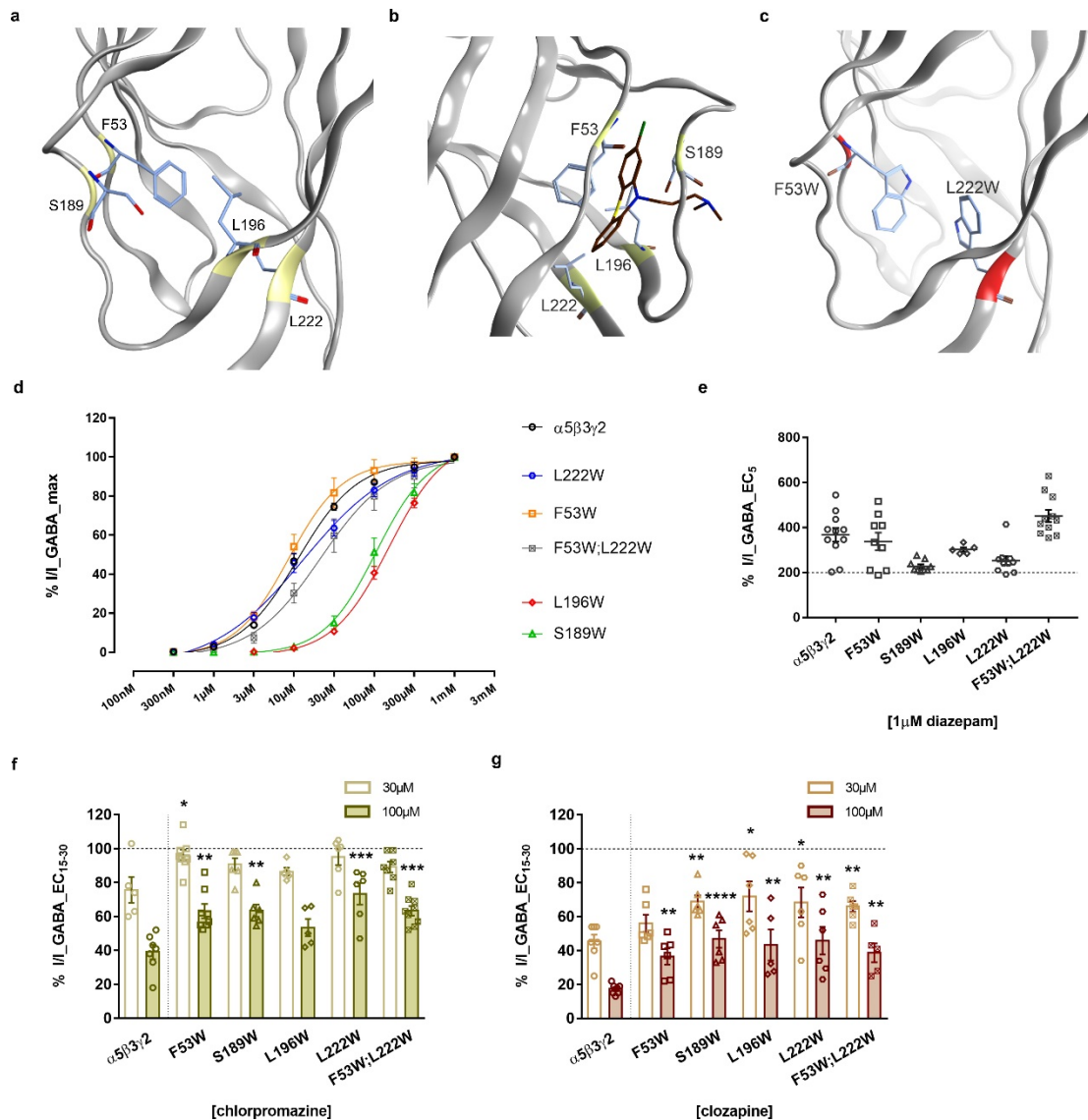


**Figure 4. Mutational analysis of the putative binding site in the  $\alpha 5$  subunit impacts on CPZ and CLZ effects.** (a-c) Binding site region of the  $\alpha 5$  subunit of the GABA<sub>A</sub> receptor (a), the same region from another perspective with CPZ docked (b), highlighting the residues subjected to mutational analysis, namely F53, S189, L196 and L222, as well as highlighting the two residues that were mutated to tryptophanes (W) (c). One chain of the protein is represented by grey ribbon. Residues to be mutated are additionally labeled and represented by licorice structures in light blue. CPZ is represented in brown as a licorice structure. Hydrogen atoms are not displayed. (d) GABA dose response curves in  $\alpha 5\beta 3\gamma 2$ ,  $\alpha 5\text{F53W}\beta 3\gamma 2$ ,  $\alpha 5\text{S189W}\beta 3\gamma 2$ ,  $\alpha 5\text{L196W}\beta 3\gamma 2$ ,  $\alpha 5\text{L222W}\beta 3\gamma 2$  and  $\alpha 5\text{F53W};\text{L222W}\beta 3\gamma 2$  receptors. Data were normalized and fitted to the Hill equation using non-linear regression and points are depicted as mean  $\pm$  SEM. Each data point represents experiments from  $n = 4-7$  oocytes from  $\geq 2$  batches. (e) Modulation of currents

elicited by an EC<sub>5</sub> GABA concentration by 1 μM diazepam. Sufficient positive allosteric modulation by 1 μM diazepam was achieved for all tested cells (above 200% which is represented by a dotted line). (f, g) Modulation of currents elicited by an EC<sub>15-30</sub> GABA concentration by 30 and 100 μM CPZ (f), as well as by 30 and 100 μM CLZ (g) in α5β3γ2 wild-type receptors, as well as in α5F53Wβ3γ2, α5S189Wβ3γ2, α5L196Wβ3γ2, α5L222Wβ3γ2 and α5F53W;L222Wβ3γ2 mutated receptors. Columns for each receptor subtype depict mean ± SEM and represent experiments from n = 5-9 oocytes from ≥2 batches. Statistically significant differences were determined for each concentration applied between mutated and wild-type receptors by two-tailed students *t*-test, where *p* < 0.05; \*\*\*\**p* < 0.0001; \*\*\**p* < 0.001; \*\**p* < 0.01; \**p* < 0.05.

CLZ and CPZ effects were measured in all five recombinantly expressed mutated receptors in order to assess whether the mutants had any impact on compound effects. CPZ and CLZ exert a strong reduction of currents in an α5-containing subtype (Figures 2b and 4f). CLZ NAM effects were observed to be significantly reduced in all receptors with each of the single mutations (Figure 4e), while the CPZ effect is diminished significantly in α5F53Wβ3γ2, α5S189Wβ3γ2 and α5L222Wβ3γ2 (Figure 4f). In the double mutant α5F53W;L222Wβ3γ2, CPZ and CLZ effects were observed to be significantly reduced, but not completely abolished (Figure 4f, g). The data suggests that CPZ and CLZ mediate a large fraction of their NAM effect via this site.

### Investigation of additional tricyclic compounds

Different studies accumulated over the years showed CLZ and several other antipsychotic and antidepressant drugs to fully or partially inhibit GABA<sub>A</sub> receptors<sup>14,15,24,27,37</sup>. Most of the prior work was done in membrane preparations from rodent brains. We, therefore, chose to test some compounds that were already investigated in radioligand binding assays by Squires and Saederup in the 80s and 90s but in a subtype specific manner. As our results have shown so far, CLZ and CPZ seem to have very similar pharmacological profiles, making it interesting to explore more compounds with similar chemical properties. Additional tricyclic compounds with comparable chemical structures to CLZ and CPZ were tested, namely levomepromazine (LEVO), imipramine (IMI), nortriptyline (NOR), loxapine (LOX) and clotiapine (CLOT) (Figure 5a).

All of these compounds share a cyclic scaffold composed of two benzene rings flanking a central, non-aromatic 6- or 7-membered ring with a substituent that carries a terminal amino group. For a more in-depth investigation of structural and stereoelectronic similarities between the selected compounds we performed pairwise shape alignments using the software ROCS<sup>38</sup>. ROCS optimizes the 3D overlay of two molecular structures in a way such that the total Van der Waals volume overlap of the atoms and the match of common chemical features is maximized. The generated output is a ranked list of best scoring alignment poses for a set of input molecules relative to one or more specified reference structure(s). For the scoring and ranking of the generated alignment poses several scoring functions are available that take shape and/or chemical feature overlap into account. We chose the most commonly used shape and color (pharmacophoric features are called 'color' features in ROCS) Tanimoto scores for our analyses (Supplementary Table S3). These scores have values ranging from 0 to 1 where 0 means no overlap at all and 1 means a perfect match. A combination of shape and color score is the Tanimoto Combo score which ranges from 0 to 2 and represents the sum of both scores (Figure 5b). The shape, color and combined shape/color similarity scores which were finally obtained for every compound pair (Figure 5b, Supplementary Table S3). For the identification of compound pairs with high mutual similarity a combo score threshold value of 1.6 was chosen.

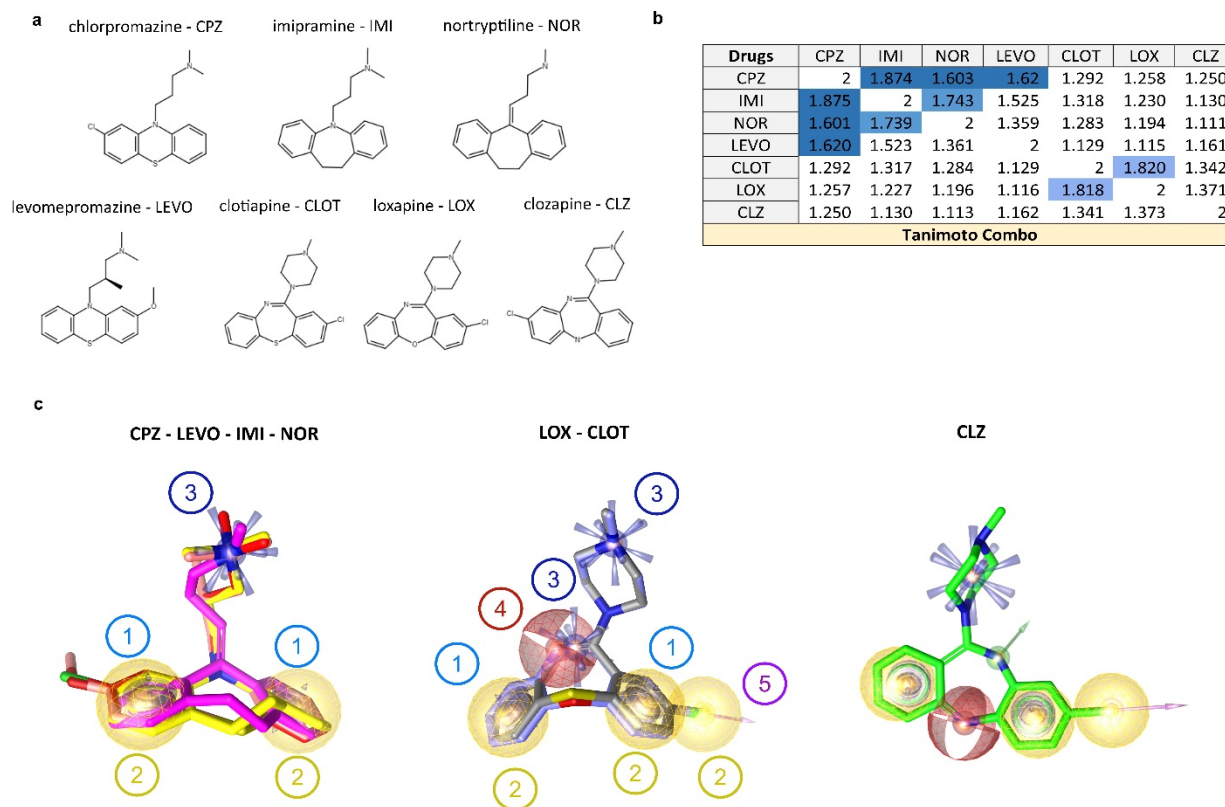


**Figure 5. Chemical structures of all drugs investigated in this study and similarity scores based on shape and pharmacophore features.** (a) Chemical structures of clozapine, chlorpromazine, levomepromazine, imipramine, nortriptyline, loxapine and clotiapine (and their abbreviations). (b) Table depicting the Tanimoto Combo similarity scores representing the sum of shape and color scores as calculated by ROCS. Individual shape and color scores can be found in Supplementary Table S3. (c) Ligand-based shared feature pharmacophores generated by LigandScout for the ligand clusters that emerged from the combo score table in panel b, as well as the pharmacophore of CLZ. Features: 1 – aromatic (blue donuts), 2 – hydrophobic (yellow spheres), 3 – positive ionizable (blue stars/rays), 4 – hydrogen bond acceptor (red sphere), 5 – halogen bond donor (magenta arrow)

This analysis revealed two groups (CPZ, IMI, NOR, LEVO; and LOX, CLOT) (Figure 5b). CLZ seems to not fall into any group and shares less pronounced similarities with both (Supplementary Figure S5). IMI and NOR form a subgroup within the first group of compounds with shape and pharmacophore similarities. For a more in-depth investigation of ligand similarities in terms of common chemical features and the resulting receptor interaction capabilities, we generated ligand-based pharmacophore models for both ligand groups using the software LigandScout (<http://www.inteligand.com/ligandscout>)<sup>39,40</sup>. A comparison of the derived shared feature pharmacophore models revealed several differences between the two ligand groups. More specifically, the cluster comprising CPZ-LEVO-IMI-NOR has two hydrophobic, two aromatic and one positive ionizable feature (Figure 5c). The second cluster consisting of LOX-CLOT contains additional features, namely one extra hydrophobic, one extra positive ionizable, one hydrogen bond acceptor and one halogen bond donor feature (Figure 5c). CLZ, as suggested by the scores in Figure 5b, shares more features with the second cluster (LOX-CLOT) and namely three hydrophobic, two aromatic, one positive ionizable and one halogen bonding feature (Supplementary Figure S5). The features that CLZ shares with the cluster CPZ-LEVO-IMI-NOR are the minimum amount of features shared by all drugs, namely two hydrophobic, one aromatic and one positive ionizable feature. Details about the mapping of the generated pharmacophore model features to ligand substructures can be found in Supplementary Table S4. The overall shape similarity is high across all seven compounds, and thus suggestive of shared targets. The clusters which share higher shape and feature similarities will likely have more targets in common.

To obtain a computational prediction for the CPZ pocket, we performed structure based pharmacophore screens of the seven compounds with two different programs (see Methods). In line with their clustering in chemical space, LOX and CLOT did not match the CPZ bound state pharmacophore with the MOE screen, and were ranked lowest with Ligand Scout. Both methods resulted in matches for CPZ, IMI, NOR and LEVO to the CPZ bound state model.

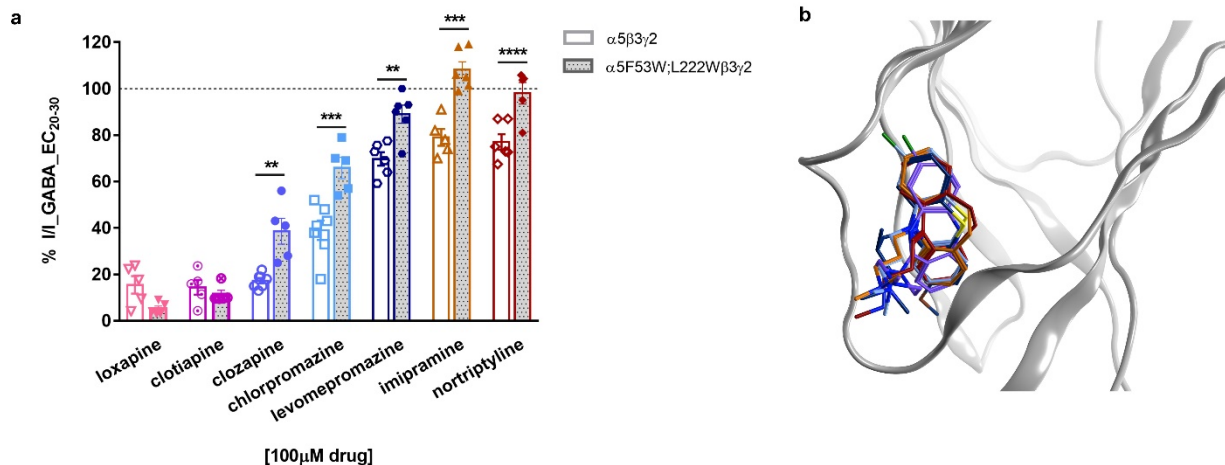


**Figure 6. Effects of all tricyclic compounds in the  $\alpha 5$  subunit double mutant.** (a) Modulation of currents elicited by an  $EC_{20-30}$  GABA concentration by 100  $\mu M$  LEVO, IMI, NOR, LOX and CLOT in  $\alpha 5\beta 3\gamma 2$  wild-type receptors, as well as in  $\alpha 5F53W;L222W\beta 3\gamma 2$  mutated receptors. CLZ and CPZ effects as in Figure 4 are depicted for direct comparison. Columns depict mean  $\pm$  SEM and represent experiments from  $n = 5-9$  oocytes from  $\geq 2$  batches. Statistically significant differences were determined for each compound between mutated and wild-type receptors by two-tailed students  $t$ -test, where  $p < 0.05$ ; \*\*\*\* $p < 0.0001$  \*\*\* $p < 0.001$ ; \*\* $p < 0.01$ . (b) CPZ docking and results of the pharmacophore screen in the  $\alpha 5$  subunit. CPZ in pink, CLZ in cyan, LEVO in yellow, NOR in green, IMI in blue (based on PDB ID: 6A96).

Next, we investigated the double mutant effects with the five additional compounds. The NAM effect elicited by LOX and CLOT is not influenced by the double mutant at all, while for CPZ, CLZ, LEVO, IMI, NOR the double mutant reduces it (Figure 6a). The latter mentioned drugs, namely CPZ, CLZ, LEVO, IMI and NOR, seem to be utilizing this site on  $\alpha 5$ -containing receptors to partially or fully exert their effect. The pharmacophore screen into the computational docking of CPZ in an  $\alpha 5$  subunit (Figure 6b) and the ligand feature-based clustering predicted the observed outcome. In order to ascertain that we don't overlook differences for LOX and CLOT at submaximal compound concentrations, we repeated the experiments at additional compound concentrations and also saw no effect of the double mutant (Supplementary Figure S6). In total, the data suggests that a CPZ site homologous to the one described in ELIC exists in the  $\alpha 5$  subunit of  $GABA_A$  receptors and it mediates a large fraction of the NAM effects elicited by IMI, NOR, CPZ, CLZ and LEVO.

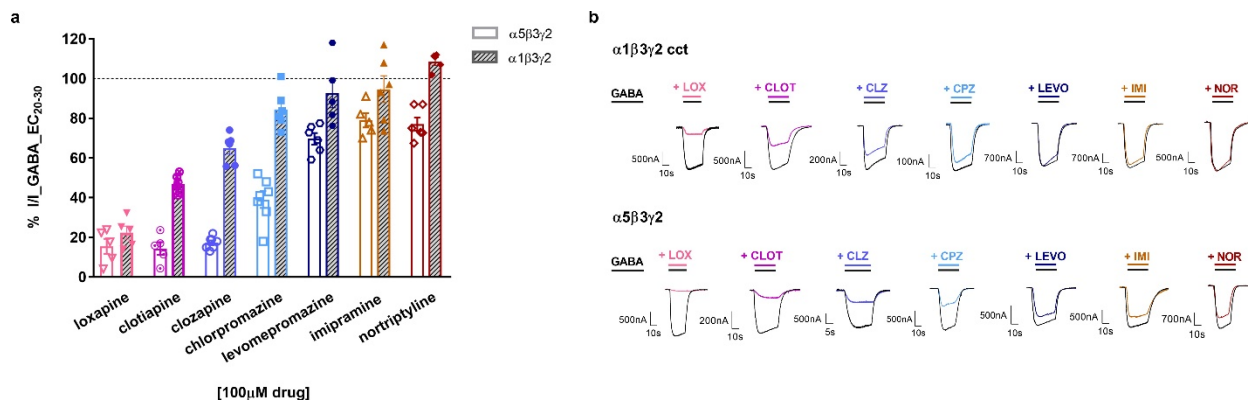


**Figure 7. Comparison of tricyclic compound effects in two wild-type receptors. (a)** Modulation of currents elicited by an EC<sub>20-30</sub> GABA concentration by 100 μM CLZ, CPZ, NOR, IMI, LEVO, LOX and CLOT in α5β3γ2 and in concatenated α1β3γ2 wild-type receptors. Data in α5β3γ2 receptors are the same as in Figure 6, reproduced here for the comparison with α1β3γ2 wild-type receptors. Columns for each receptor subtype depict mean ± SEM and represent experiments from n = 5-9 oocytes from ≥2 batches. Statistically significant differences were determined for each compound between mutated and wild-type receptors by two-tailed students *t*-test, where *p* < 0.05; \*\*\*\**p* < 0.0001 \**p* < 0.05. **(b)** Representative traces from electrophysiological recordings of LOX, CLOT, CLZ, CPZ, LEVO, IMI and NOR co-applied with GABA in α1β3γ2 (concatenated) and α5β3γ2 receptors.

For both CPZ and CLZ we observed a strong impact of the alpha isoform on efficacy. Since α1βγ2 is the most abundant subunit combination in the mammalian brain and has been claimed to mediate drug induced seizures<sup>41</sup>, we completed the dataset for the remaining compounds with the α1β3γ2 receptor (Figure 7). NOR and IMI are inactive in this subtype, LEVO, CPZ, CLZ and CLOT exert less NAM efficacy compared to the α5-containing combination, and LOX modulates both to the same high extent. Thus, the chemotypes represented by these seven compounds display moderate potential for alpha- isoform selective targeting. The compounds, with the exception of LOX, generally favour the α5-containing over α1-containing subtypes, which is relevant for a favourable toxicological profile.

## Discussion

We have demonstrated negative modulation of α5β3γ2 receptors by seven compounds which share shape and pharmacophore similarity. The observed efficacies range from very weak (IMI and NOR) to very strong current reduction for CLZ, LOX and CLOT. Interactions of all compounds with GABA<sub>A</sub> receptors, with the exception of LEVO, were previously noted, but the binding sites remained elusive<sup>14,15,42</sup>. Thus, inspired by a CPZ site in the ECD of a bacterial GABA-gated channel, we employed mutational analysis to probe the existence of a homologous “CPZ pocket” in α5 subunits. Interestingly, five of the seven compounds we tested respond with a clear reduction of function to multiple mutants in the pocket. Gratifyingly, the two compounds which form a separate cluster in pharmacophore feature space (LOX, CLOT) are insensitive to the tested mutants, which suggests that they use a distinctive site. Alternatively, since this newly described pocket is of relatively large size, it is also possible that the mutations do not fully occlude the site, making it still accessible by the ligand in certain conformations. Incomplete occlusion of the pocket might also explain why the double mutant failed to abolish the CPZ effect completely, while the elimination of the α5 subunit does. Further studies with direct structural methods seem warranted to further clarify the usage of binding sites by these and other related molecules.

Negative modulation of hippocampal α5β3γ2 receptors has been studied exhaustively in preclinical studies<sup>6,43</sup>. The key role that this receptor population plays in multiple aspects of memory and cognitive performance has led to the development and subsequent clinical trial of basmisanil. This compound, previously known as RG-1662 or RO5186582, is also an allosteric negative modulator of α5βγ2 receptors and has been under evaluation as an

adjunctive therapy in a schizophrenic cohort for the treatment of cognitive impairment associated with schizophrenia, unfortunately with negative outcome (<https://clinicaltrials.gov/ct2/show/NCT02953639>). It is unlikely that the contribution of hippocampal  $\alpha 5$ -containing receptors to cognitive performance is radically different in humans compared to laboratory animals, thus, the failure of basmisanil is probably not a failure of translational validity. The negative results of the clinical trial could possibly be explained by a recent study that compared basmisanil with other  $\alpha 5$ -NAMs and found it markedly less potent than all other  $\alpha 5$ -NAMs tested<sup>44</sup>. Alternative explanations could be tolerance development as basmisanil targets the benzodiazepine site, and most benzodiazepine drugs induce tolerance<sup>45,46</sup>. It is important to note that all  $\alpha 5$ -NAMs that were developed so far target the benzodiazepine binding site, while the compounds we study here have been known to display negligible affinities to this site, and the NAM effect of CLZ and CPZ is independent of the presence of the  $\gamma 2$  subunit which forms part of the benzodiazepine site. CLZ elicits its  $\alpha 5$ -NAM effect under in vitro conditions in the micromolar range. As previously investigated, plasma concentrations of CLZ can reach up to 3 $\mu$ M in CLZ-responding patients with schizophrenia<sup>24</sup>. Another study shows that in rat, and likely also in human, the concentration of CLZ can be 24-fold higher in the brain compared to the plasma concentrations<sup>24</sup>. Therefore, the therapeutic concentrations of CLZ in the brain can be in the high micromolar range, which would make the concentrations used in this study physiologically relevant. For CLZ and many other antipsychotics, high doses are needed to produce a therapeutic effect. It was already questioned by Squires and Saederup in the nineties<sup>24</sup> if these high doses are consistent with their antipsychotic effects by means of dopamine, serotonin, adrenergic or histaminergic receptors, for which  $K_i$  values are in the low nanomolar range<sup>17</sup>.

Our main focus was on CLZ, which has long been argued to mediate at least parts of its therapeutic effects by so far unknown targets<sup>47</sup>. Of note, the combined findings of this study and other work<sup>22</sup> clearly demonstrate that CLZ is not an  $\alpha 5$ -selective NAM. It interacts with a multitude of GABA<sub>A</sub> receptor subtypes, with a relatively weak NAM effect in  $\alpha 1$ -containing receptors (see Figure 7), but e.g.  $\alpha 2$ -containing receptors are also strongly modulated (see Fig 1). Over the years GABA<sub>A</sub> receptors have been understood as a large family, with each of the 19 subunits contributing unique properties to the pentameric assemblies in which they are integrated. Historically, it was felt that a large fraction of the receptors might contribute to therapeutic effects of antipsychotics<sup>48,49</sup>, and GABA<sub>A</sub> receptor targeting drugs were even considered as monotherapy<sup>50</sup>. Moreover, extensive alterations of GABA<sub>A</sub> receptor subunit expression in diverse brain regions have been observed in post mortem studies of schizophrenia<sup>51</sup>, pointing to the involvement of multiple subtypes in the psychopathology. Beyond the hippocampal  $\alpha 5$ -containing receptors it thus still remains unclear which GABA<sub>A</sub> receptor subtypes in which brain circuits may prove to be useful targets. In fact, the benzodiazepine site ligand bretazenil which was found to be moderately effective as antipsychotic monotherapy<sup>50</sup> is not subtype selective<sup>52</sup>. It thus seems important to examine the GABA<sub>A</sub> subtype profiles of antipsychotic compounds side by side with similar compounds which lack antipsychotic efficacy to generate an evidence based list of interesting subtypes based on human data.

It is interesting to interpret our findings with the recombinantly expressed receptor subtypes in the light of earlier radioligand assay studies performed with rodent brain membranes by Squires and Saederup. We observe no modulatory effects by IMI and NOR in the most abundant receptor subtype. The studies by Squires and Saederup did not examine current modulation, but the modulation of GABA inhibition of [<sup>35</sup>S]TBPS binding<sup>37</sup>, which is also a very sensitive indicator for allosteric binding sites. In their work they also found IMI and NOR nearly inactive, fully consistent with our results. Squires and Saederup also performed “additivity studies” using CLZ co-applied with other antipsychotics<sup>15</sup>. Among the drugs tested together with CLZ were LOX and CLOT, both of which had a significantly additive effect when co-applied with CLZ compared to the effect of CLZ alone. This is suggesting action on either distinctive subtypes, or different binding sites. In line with these observations, we find CLZ partially responsive to the double mutant, while LOX and CLOT are not. While the two studies cannot be compared directly, the degree of

consistency is intriguing and points further to the need for more subtype profiles of antipsychotic drugs that were shown to interact with GABA<sub>A</sub> receptors.

To further address the question how the GABA<sub>A</sub> receptor modulation observed by us and others which is elicited by CLZ may contribute to specific wanted and unwanted effects, it seems helpful to take a broader perspective on the circuitries that are implicated in schizophrenia. Schizophrenia is in fact a very broad diagnostic entity and presents with many symptoms. Accumulated evidence suggests a complex, likely multicausal etiology of the pathogenetic mechanisms that drive schizophrenia symptoms, involving several neurotransmitter systems including dopamine, GABA and glutamate<sup>53</sup>. Up to 30% of patients with schizophrenia show no or only partial response to treatment with at least two different antipsychotic medications<sup>54</sup>. In those patients, the atypical antipsychotic CLZ was undoubtedly confirmed to be the single most effective treatment choice, providing additional relief from some negative symptoms compared to other antipsychotics. Therefore, CLZ was the first agent to challenge the prevailing notion of potent dopamine D2 antagonism as a premise for antipsychotic efficacy<sup>55</sup> and it is still the most effective medication compared to typical antipsychotics, as well as for schizophrenia patients who are treatment resistant<sup>16</sup>.

The search for a single target or even a single pathway has gradually given way to a more integrated view on antipsychotic therapy. Antipsychotic drugs, and also many antidepressants display very pronounced polypharmacology, prompting us to carefully examine the current knowledge as reflected in DrugCentral. We integrated the results from this study into the profiles of the seven tested compounds (Figure 8 and Supplementary Figure S7, Supplementary Table S5). Figure 8 reflects the fact that an interaction between the drug and the target has been observed, but not the affinity or the effect the drug has on any of the targets, it can be conceptualized as a qualitative interactome.

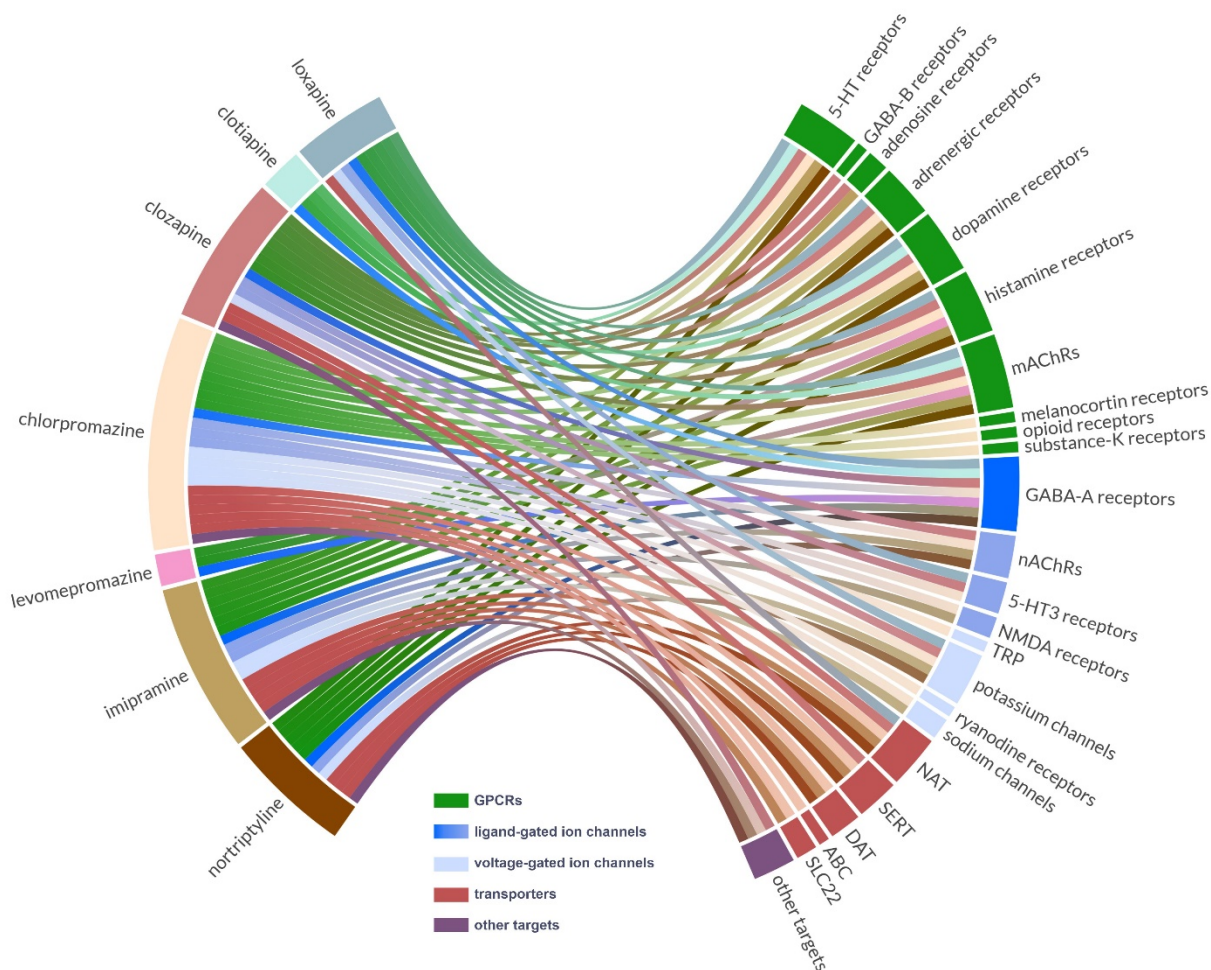


**Figure 8. Drug- target interactions.** Chord diagram showing the drugs tested in this study and their known targets (G-protein-coupled receptors, ligand-gated ion channels, ion channels, transporters and other targets) grouped according to the IUPHAR recommended categories. The drugs are ordered by decreasing  $\alpha$ 5-NAM efficacy, the targets are ordered to reflect IUPHAR categories. A more detailed diagram can be found in Supplementary Figure S7.

In terms of their clinical use, the seven compounds can be grouped into the antipsychotics LOX, CLOT, CLZ and CPZ, LEVO is considered as weak antipsychotic with strong sedative effects, while IMI and NOR are tricyclic antidepressants. In line with the high similarity among these compounds in chemical space, their target profiles overlap broadly with no clear signature that would set the antidepressants apart from the antipsychotics. Intriguingly, the  $\alpha$ 5-NAM effects we report are much stronger for the antipsychotic compounds and relatively weak for the antidepressants. The polypharmacology of all these drugs poses a considerable challenge in the study of their mechanism of action. At the same time, beneficial polypharmacology has been widely acknowledged and is thought to be much more widespread than currently known<sup>56</sup>. As evidenced by efforts to combine antipsychotic medications<sup>57,58</sup> to improve treatment outcome, the effects of individual compounds may add up in synergistic ways, and thus a diversity of targets may contribute to therapeutic outcome<sup>56</sup>. This suggests that “beneficial polypharmacology” can be conceptualized as interactions of a drug with a group of targets that form a therapeutic portfolio. The notion of combined influences on targets from multiple neurotransmitter systems thus may consolidate the dopamine, glutamate and GABA hypotheses into a unified disbalance hypothesis<sup>59</sup>. Not only GABA<sub>A</sub> receptors have been under scrutiny, but CLZ’s action on GABA<sub>B</sub> receptors has also been proposed as a promising

lead<sup>60</sup>. Thus, the tentative role of hippocampal and other GABA receptor populations in such a therapeutic portfolio await to be clarified. It seems important that the knowledge on drug interactions with defined subtypes of ligand gated ion channels is advanced, such data still is largely lacking (Supplementary Table S6).

While further research will be needed to firmly link specific and identified GABA<sub>A</sub> receptor subtypes with specific therapeutic outcomes, it is interesting to interpret our findings in terms of potential advances for rational drug development. The design of drugs that display wanted polypharmacology is still in its infancy<sup>61</sup>. The intrasubunit CPZ site we identified here does not coincide with the binding sites used by classical GABA<sub>A</sub> receptor targeting drugs such as benzodiazepines. This difference in binding site localization has important implications: Targeting the benzodiazepine binding site will result in unwanted interference with benzodiazepine medications. In contrast, drugs targeting the novel CPZ site might confer reduced liability to antagonize other GABA<sub>A</sub> targeting therapeutic effects such as anxiolysis.

Interestingly, antipsychotic drugs which hit many targets often display low or no affinity for the benzodiazepine site<sup>59</sup>. The novel site we describe here is also likely to exist in nicotinic acetylcholine receptors (nAChRs) since notably CLZ also potently inhibits  $\alpha$ 7-nAChRs<sup>62</sup>. Interestingly, a “dual modulator” that acts both as an  $\alpha$ 5 GABA<sub>A</sub>R-NAM and as an  $\alpha$ 7 nAChR-PAM has been investigated in animal models and showed that it can have positive effects in behavioral tests that measure attentional capacity, spatial learning and memory<sup>61</sup>. Thus, compounds akin to CLZ may inherently target such sites in the family of pentameric ligand gated ion channels.

In conclusion, existing evidence strongly suggests a “therapeutic portfolio” mode of action of antipsychotic medications. The exact configuration of an antipsychotic target portfolio remains to be elucidated and likely will contain both metabotropic and ionotropic receptors (Figure 8). Hippocampal  $\alpha$ 5-containing GABA<sub>A</sub> receptors are strong candidates, and strongly modulated by the antipsychotics we tested. Molecules which hit “classical” targets such as D2 receptors and GABA<sub>A</sub> receptors via the newly described intrasubunit site may thus be an attractive alternative to the strategy that drove the development of basmisanil, namely to augment antipsychotics with GABA-ergics.

## Materials

*Xenopus laevis* oocytes were commercially purchased from Ecocyte Biosciences. Compounds purchased from Sigma Aldrich were: GABA (A2129-100g), Chlorpromazine (C8138-5g), Imipramine (I7379-5g) and Loxapine (L106-100mg), from Biomedica Medizinprodukte: Clozapine (RD 0444/50), from THP Medical products: Levomepromazine (MCE-HY-B1693-100mg), Nortriptyline (T1327-200mg), from Szabo-Scandic Handels: Clothiapine (SACSC-200404A) and all other chemicals were purchased from Sigma Aldrich.

## Methods

### Functional Testing with Two Electrode Voltage Clamp (TEV) in *Xenopus laevis* Oocytes

Stock solution and buffers were prepared as described in Simeone et al. For the electrophysiological experiments, GABA was dissolved in NDE buffer with a concentration in order to achieve the appropriate EC concentration relevant to each experiment. In brief, all other compounds were dissolved in DMSO with a stock concentration of 100mM (except Clotiapine in 25mM) and for further dilutions, the compounds were diluted in NDE plus GABA (EC<sub>x</sub>).

The mutated rat  $\alpha 5$  GABA<sub>A</sub> receptor subunit cDNA constructs were purchased from Eurofins Genomics. The company performed the cloning by the use of site directed mutagenesis on a rat  $\alpha 5$  insert in a pCI vector which was provided by us. The following constructs were created:  $\alpha 5F53W$ ,  $\alpha 5S189W$ ,  $\alpha 5L196W$ ,  $\alpha 5L222W$  and  $\alpha 5F53W;L222W$  (numbering without signal peptide) and were validated by double stranded DNA sequencing.

In order to generate mRNA, all constructs were linearized, transcribed and purified as described previously<sup>63</sup>. For the microinjection, the RNA of  $\alpha\beta$  receptor combinations was mixed at 1:1 ratio and  $\alpha 1,2\beta\gamma$  receptors were mixed at 1:1:5 ratio, whereas  $\alpha 5\beta\gamma$  receptors were mixed at 3:1:5 ratio. The approach used for subunit concatenation of  $\alpha 1\beta 3\gamma 2$  GABA<sub>A</sub> receptors has been described previously<sup>64</sup>. The dual ( $\gamma 2\beta 3$ ) and triple ( $\alpha 1\beta 3\alpha 1$ ) constructs were injected at a ratio of 1:1<sup>64</sup>.  $\beta 2\gamma 2$  receptors were mixed with a 1:3 ratio, as described in Wongsamitkul et al<sup>65</sup>. The RNA for the  $\alpha 5(\text{mut})\beta 3\gamma 2$  receptor was mixed at 3:1:5 ratio, as for the wild-type  $\alpha 5\beta 3\gamma 2$ , with a final concentration of 70 ng/ $\mu\text{l}$ .

Healthy defolliculated oocytes were injected with an aqueous solution of mRNA with a Nanoject II (Drummond). The injected oocytes were incubated at 18 °C (ND96 + antibiotic) for 2-3 days for  $\alpha\beta$  receptors and for 3-4 days for  $\alpha\beta\gamma$  receptors before recording. Electrophysiological recordings were performed as specified in Simeone et al<sup>63</sup>. A GABA concentration amounting to 5–10% of maximum GABA currents is termed EC<sub>5-10</sub> (accordingly 20-30% of maximum GABA currents is EC<sub>20-30</sub>, 15-30% of maximum GABA currents is EC<sub>15-30</sub> etc.). In Figure 1e, experiments with the neurosteroid THDOC were performed. The two columns on the right y axis represent the two types of experiments performed, namely only co-application of CLZ with THDOC, as well as pre-application of CLZ right before CLZ and THDOC co-application (Figure 1e). To ensure the incorporation of the  $\gamma 2$  subunit, diazepam was applied at the end of each screening (~200% at 1 $\mu\text{M}$ ). All recordings were performed at room temperature at a holding potential of -60 mV using a Dagan TEV-200A two-electrode voltage clamp (Dagan Corporation).

## Computational Modeling and Docking

Structural superpositions were performed with the PDBeFold webserver (<http://www.ebi.ac.uk/msd-srv/ssm/>) and further processed with MOE (<http://www.chemcomp.com>). Pocket volumes were calculated with Conolly, as implemented in MOE. Loop F remodeling was performed using Modeller<sup>66</sup> (<https://salilab.org/modeller/>) and based on the sequence alignment depicted in Figure 3.

Molecular Docking was performed using GOLD 5.7.1<sup>67</sup> after appropriate preparation of protein and ligands. The centroid of the binding site was chosen by the position of the sulfur from the CPZ of 5LG3 after it was superposed with the alpha-5 subunit of 6A96 with a binding site radius of 10Å. On the protein, loop F steric restraints were disabled (V181-Y191 in 6D6T chain X and V184-Y194 in 6A96, chain A) and the sidechains displayed in Figure 3 were set flexible for the docking runs. The 100 poses were generated for each run in which the ligands Ring-NR1R2 was set flexible and the generation of diverse solutions was enabled. The goldscore was used as the primary scoring function (default).

## Ligand Analysis and Pharmacophore Modeling

For every ligand a conformer ensemble was generated using OMEGA 3.1.1.2 (OpenEye Scientific Software, Santa Fe, NM, USA. <http://www.eyesopen.com>)<sup>68</sup> applying default settings for all parameters and output in SD-format. Shape and color similarity scores were calculated using ROCS 3.3.1.2 (OpenEye Scientific Software, Santa Fe, NM, USA. <http://www.eyesopen.com>)<sup>38</sup> with the -mcquery parameter set to true and applying default settings for all other

parameters. The same combined multi-conf. SD-file of all ligands was specified both as input file for the query structures and the screened molecule database. The pairwise Shape Tanimoto, Color Tanimoto and Tanimoto Combo scores calculated for a particular ligand were then extracted from the corresponding ROCS CSV output file that was generated for this ligand.

Ligand-based pharmacophore models of the identified ligand clusters were generated using LigandScout 4.4 (Inte:Ligand GmbH, Vienna, Austria. <http://www.inteligand.com/ligandscout>)<sup>39,40</sup>. In the ligand-based modeling perspective, all ligands constituting a cluster were added to the training-set and then conformers were generated using iCon<sup>69</sup> in FAST mode but with the RMSD threshold set to 0.35 to obtain denser conformer ensembles. Ligand-based model generation was performed with the output pharmacophore type set to 'Shared feature pharmacophore' and default settings for all other parameters.

Structure-based 3D pharmacophore screening of CLZ, IMI, CLO, NOR, LEVO and LOX was performed into the  $\alpha 5$  subunit with the CPZ docking result depicted in Figure 4b using MOE 2019.0102 and LigandScout 4.4. For LigandScout the "Pharmacophore-Fit" scoring function with the "match all query features" screening mode was used with exclusion spheres enabled and a maximum of one omitted feature. In MOE the unified pharmacophore algorithm was used with at least six pharmacophore-features to match. For both programs the pharmacophore-features were automatically generated and the default settings were used with the exception of the omitted features which were changed manually.

## Data analysis and Figure generation

Data was recorded and digitized using an Axon Digidata 1550 low-noise data acquisition system (Axon Instruments). Data acquisition was performed using pCLAMP v.10.5 (Molecular Devices™). The same programme was used for the processing of representative traces, which were later visualized using GraphPad Prism (v.6.). Data were analysed using GraphPad Prism (v.6.) and plotted as concentration-response curves or column graphs, as defined in Simeone et al<sup>63</sup>. Figures of concentration-response curves and column graphs were generated using GraphPad Prism (v.6.). These curves were normalized and fitted by non-linear regression analysis to the equation  $Y = \text{bottom} + (\text{top} - \text{bottom}) / (1 + (\text{IC}_{50}/X)^{nH})$ , where  $\text{IC}_{50}$  is the concentration of the compound that decreases the amplitude of the GABA-evoked current by 50%, and  $nH$  is the Hill coefficient. Structural images were generated using MOE, while images with pharmacophore models using LigandScout 4.4.

For the chord diagram, DrugCentral (<https://drugcentral.org/> accessed on 06.01.2020) was used and only mammalian drug targets were taken into account. Additionally, for GABA<sub>A</sub> and GABA<sub>B</sub> as well as for nAChRs, literature findings were added (Supplementary Table S6)<sup>14,15,22,30,42,62,70-73</sup>. Terminology was unified across all drug targets (since differences exist, e.g. Serotonin (5-HT<sub>3</sub>) receptor 3 and 5-hydroxytryptamine receptor 3). Targets were grouped according to the IUPHAR recommended categories. The chord diagram was created with python 3.8 and the python package chord (<https://pypi.org/project/chord/>).

## Statistics

All data are expressed as mean  $\pm$  SEM and were analyzed using a two-tailed Student's t-test. One sample t-test was performed in order to determine statistical significance of each mean response from control current. A p-value less than 0.05 was considered statistically significant, where \*\*\*\*p < 0.0001, \*\*\*p < 0.001, \*\*p < 0.01, \*p < 0.05 and n.s. p > 0.05. All statistical tests that have been used, and applied to sample sizes in the study, are indicated in the

figure legends. The n number stated represents the number of single oocyte experiments. The exact n values are reported by the individual values shown in all scatter plot bar graphs, as well as in the figure legends. All data subjected to statistical analysis have a group size of (n) ≥ 5. Statistical analysis was performed using GraphPad Prism (v.6.).

## Data availability

The datasets generated and/or analyzed during the current study are available from the corresponding author upon request.

## References

1. Lieberman, J.A. et al. Hippocampal dysfunction in the pathophysiology of schizophrenia: a selective review and hypothesis for early detection and intervention. *Molecular Psychiatry* **23**, 1764-1772 (2018).
2. Lodge, D.J. & Grace, A.A. Hippocampal dysregulation of dopamine system function and the pathophysiology of schizophrenia. *Trends Pharmacol Sci* **32**, 507-13 (2011).
3. Nakahara, S., Matsumoto, M. & van Erp, T.G.M. Hippocampal subregion abnormalities in schizophrenia: A systematic review of structural and physiological imaging studies. *Neuropsychopharmacol Rep* **38**, 156-166 (2018).
4. Skilbeck, K.J., O'Reilly, J.N., Johnston, G.A.R. & Hinton, T. The effects of antipsychotic drugs on GABAA receptor binding depend on period of drug treatment and binding site examined. *Schizophrenia research* **90**, 76-80 (2007).
5. Marques, T.R. et al. GABA-A receptor differences in schizophrenia: a positron emission tomography study using [11C]Ro154513. *Molecular Psychiatry* (2020).
6. Xu, M.-y. & Wong, A.H.C. GABAergic inhibitory neurons as therapeutic targets for cognitive impairment in schizophrenia. *Acta Pharmacologica Sinica* **39**, 733-753 (2018).
7. Lingford-Hughes, A. et al. Imaging the GABA-benzodiazepine receptor subtype containing the alpha5-subunit in vivo with [11C]Ro15 4513 positron emission tomography. *J Cereb Blood Flow Metab* **22**, 878-89 (2002).
8. Etherington, L.A. et al. Selective inhibition of extra-synaptic  $\alpha$ 5-GABA(A) receptors by S44819, a new therapeutic agent. *Neuropharmacology* **125**, 353-364 (2017).
9. Gill, K.M. & Grace, A.A. The role of alpha5 GABAA receptor agonists in the treatment of cognitive deficits in schizophrenia. *Curr Pharm Des* **20**, 5069-76 (2014).
10. Knust, H. et al. The discovery and unique pharmacological profile of RO4938581 and RO4882224 as potent and selective GABAA alpha5 inverse agonists for the treatment of cognitive dysfunction. *Bioorg Med Chem Lett* **19**, 5940-4 (2009).
11. Sigel, E. & Ernst, M. The Benzodiazepine Binding Sites of GABAA Receptors. *Trends Pharmacol Sci* **39**, 659-671 (2018).
12. Atack, J.R. et al. L-655,708 enhances cognition in rats but is not proconvulsant at a dose selective for alpha5-containing GABAA receptors. *Neuropharmacology* **51**, 1023-9 (2006).
13. Glykys, J., Mann, E.O. & Mody, I. Which GABA(A) receptor subunits are necessary for tonic inhibition in the hippocampus? *J Neurosci* **28**, 1421-6 (2008).
14. Squires, R.F. & Saederup, E. Antidepressants and metabolites that block GABAA receptors coupled to 35S-t-butylbicyclophosphorothionate binding sites in rat brain. *Brain Res* **441**, 15-22 (1988).

15. Squires, R.F. & Saederup, E. Clozapine and Several Other Antipsychotic/Antidepressant Drugs Preferentially Block the Same 'Core' Fraction of GABA<sub>A</sub> Receptors. *Neurochemical Research* **23**, 1283-1290 (1998).
16. Attard, A. & Taylor, D.M. Comparative effectiveness of atypical antipsychotics in schizophrenia: what have real-world trials taught us? *CNS Drugs* **26**, 491-508 (2012).
17. Seeman, P. Targeting the dopamine D2 receptor in schizophrenia. *Expert Opin Ther Targets* **10**, 515-31 (2006).
18. Mozrzymas, J.W., Barberis, A., Michalak, K. & Cherubini, E. Chlorpromazine inhibits miniature GABAergic currents by reducing the binding and by increasing the unbinding rate of GABA<sub>A</sub> receptors. *J Neurosci* **19**, 2474-88 (1999).
19. Schwartz, R.D. & Mindlin, M.C. Inhibition of the GABA receptor-gated chloride ion channel in brain by noncompetitive inhibitors of the nicotinic receptor-gated cation channel. *J Pharmacol Exp Ther* **244**, 963-70 (1988).
20. Seeman, P. Brain dopamine receptors. *Pharmacol Rev* **32**, 229-313 (1980).
21. Yokota, K. et al. The effects of neuroleptics on the GABA-induced Cl<sup>-</sup> current in rat dorsal root ganglion neurons: differences between some neuroleptics. *Br J Pharmacol* **135**, 1547-55 (2002).
22. Korpi, E.R., Wong, G. & Luddens, H. Subtype specificity of gamma-aminobutyric acid type A receptor antagonism by clozapine. *Naunyn Schmiedebergs Arch Pharmacol* **352**, 365-73 (1995).
23. Michel, F.J. & Trudeau, L.E. Clozapine inhibits synaptic transmission at GABAergic synapses established by ventral tegmental area neurones in culture. *Neuropharmacology* **39**, 1536-43 (2000).
24. Squires, R.F. & Saederup, E. Clozapine and some other antipsychotic drugs may preferentially block the same subset of GABA(A) receptors. *Neurochem Res* **22**, 151-62 (1997).
25. Squires, R.F. & Saederup, E. Clozapine's antipsychotic effects do not depend on blockade of 5-HT<sub>3</sub> receptors. *Neurochem Res* **24**, 659-67 (1999).
26. Squires, R.F. & Saederup, E. Mono N-aryl ethylenediamine and piperazine derivatives are GABA<sub>A</sub> receptor blockers: implications for psychiatry. *Neurochem Res* **18**, 787-93 (1993).
27. Squires, R.F. & Saederup, E. Additivities of compounds that increase the numbers of high affinity [<sup>3</sup>H]muscimol binding sites by different amounts define more than 9 GABA(A) receptor complexes in rat forebrain: implications for schizophrenia and clozapine research. *Neurochem Res* **25**, 1587-601 (2000).
28. Nys, M. et al. Allosteric binding site in a Cys-loop receptor ligand-binding domain unveiled in the crystal structure of ELIC in complex with chlorpromazine. *Proc Natl Acad Sci U S A* **113**, E6696-e6703 (2016).
29. Olsen, R.W. & Sieghart, W. International Union of Pharmacology. LXX. Subtypes of gamma-aminobutyric acid(A) receptors: classification on the basis of subunit composition, pharmacology, and function. Update. *Pharmacol Rev* **60**, 243-60 (2008).
30. Asproni, B. et al. Synthesis and pharmacological evaluation of 1-[(1,2-diphenyl-1H-4-imidazolyl)methyl]-4-phenylpiperazines with clozapine-like mixed activities at dopamine D(2), serotonin, and GABA(A) receptors. *J Med Chem* **45**, 4655-68 (2002).
31. Wohlfarth, K.M., Bianchi, M.T. & Macdonald, R.L. Enhanced neurosteroid potentiation of ternary GABA(A) receptors containing the delta subunit. *J Neurosci* **22**, 1541-9 (2002).
32. Liu, S. et al. Cryo-EM structure of the human  $\alpha 5\beta 3$  GABA(A) receptor. *Cell Res* **28**, 958-961 (2018).
33. Masiulis, S. et al. GABA(A) receptor signalling mechanisms revealed by structural pharmacology. *Nature* **565**, 454-459 (2019).
34. Phulera, S. et al. Cryo-EM structure of the benzodiazepine-sensitive  $\alpha 1\beta 1\gamma 2S$  tri-heteromeric GABA(A) receptor in complex with GABA. *Elife* **7**(2018).
35. Zhu, S. et al. Structure of a human synaptic GABA(A) receptor. *Nature* **559**, 67-72 (2018).
36. Puthenkalam, R. et al. Structural Studies of GABA-A receptor binding sites: Which experimental structure tells us what? *Frontiers in Molecular Neuroscience* **9**(2016).

37. Squires, R.F. & Saederup, E. GABAA receptor blockers reverse the inhibitory effect of GABA on brain-specific [35S]TBPS binding. *Brain Res* **414**, 357-64 (1987).
38. Hawkins, P.C.D., Skillman, A.G. & Nicholls, A. Comparison of Shape-Matching and Docking as Virtual Screening Tools. *Journal of Medicinal Chemistry* **50**, 74-82 (2007).
39. Wolber, G., Dornhofer, A.A. & Langer, T. Efficient overlay of small organic molecules using 3D pharmacophores. *J Comput Aided Mol Des* **20**, 773-88 (2006).
40. Wolber, G. & Langer, T. LigandScout: 3-D pharmacophores derived from protein-bound ligands and their use as virtual screening filters. *J Chem Inf Model* **45**, 160-9 (2005).
41. Crestani, F., Assandri, R., Täuber, M., Martin, J.R. & Rudolph, U. Contribution of the alpha1-GABA(A) receptor subtype to the pharmacological actions of benzodiazepine site inverse agonists. *Neuropharmacology* **43**, 679-84 (2002).
42. Besnard, J. et al. Automated design of ligands to polypharmacological profiles. *Nature* **492**, 215-220 (2012).
43. Prévot, T. & Sibille, E. Altered GABA-mediated information processing and cognitive dysfunctions in depression and other brain disorders. *Molecular Psychiatry* **26**, 151-167 (2021).
44. Manzo, M.A. et al. Inhibition of a tonic inhibitory conductance in mouse hippocampal neurones by negative allosteric modulators of  $\alpha 5$  subunit-containing  $\gamma$ -aminobutyric acid type A receptors: implications for treating cognitive deficits. *Br J Anaesth* **126**, 674-683 (2021).
45. Myers, J.F., Comley, R.A. & Gunn, R.N. Quantification of [ $^{11}$ C]Ro15-4513 GABA(A) $\alpha 5$  specific binding and regional selectivity in humans. *J Cereb Blood Flow Metab* **37**, 2137-2148 (2017).
46. Vinkers, C.H. & Olivier, B. Mechanisms Underlying Tolerance after Long-Term Benzodiazepine Use: A Future for Subtype-Selective GABA(A) Receptor Modulators? *Adv Pharmacol Sci* **2012**, 416864 (2012).
47. O'Connor, W.T. & O'Shea, S.D. Clozapine and GABA transmission in schizophrenia disease models: establishing principles to guide treatments. *Pharmacol Ther* **150**, 47-80 (2015).
48. Squires, R.F. & Saederup, E. A review of evidence for GABergic predominance/glutamatergic deficit as a common etiological factor in both schizophrenia and affective psychoses: more support for a continuum hypothesis of "functional" psychosis. *Neurochem Res* **16**, 1099-111 (1991).
49. Fatemi, S.H., Folsom, T.D. & Thuras, P.D. GABA(A) and GABA(B) receptor dysregulation in superior frontal cortex of subjects with schizophrenia and bipolar disorder. *Synapse* **71**(2017).
50. Delini-Stula, A. & Berdah-Tordjman, D. Antipsychotic effects of bretazenil, a partial benzodiazepine agonist in acute schizophrenia--a study group report. *J Psychiatr Res* **30**, 239-50 (1996).
51. Fatemi, S.H. & Folsom, T.D. GABA receptor subunit distribution and FMRP-mGluR5 signaling abnormalities in the cerebellum of subjects with schizophrenia, mood disorders, and autism. *Schizophr Res* **167**, 42-56 (2015).
52. Ramerstorfer, J., Furtmüller, R., Vogel, E., Huck, S. & Sieghart, W. The point mutation gamma 2F77I changes the potency and efficacy of benzodiazepine site ligands in different GABAA receptor subtypes. *Eur J Pharmacol* **636**, 18-27 (2010).
53. Charych, E.I., Liu, F., Moss, S.J. & Brandon, N.J. GABA(A) receptors and their associated proteins: implications in the etiology and treatment of schizophrenia and related disorders. *Neuropharmacology* **57**, 481-95 (2009).
54. Conley, R.R. & Kelly, D.L. Management of treatment resistance in schizophrenia. *Biol Psychiatry* **50**, 898-911 (2001).
55. Stille, G., Lauener, H. & Eichenberger, E. The pharmacology of 8-chloro-11-(4-methyl-1-piperazinyl)-5H-dibenzo(b,e)(1,4)diazepine (clozapine). *Farmaco Prat* **26**, 603-25 (1971).
56. Anighoro, A., Bajorath, J. & Rastelli, G. Polypharmacology: Challenges and Opportunities in Drug Discovery. *Journal of Medicinal Chemistry* **57**, 7874-7887 (2014).

57. Barnes, T.R. & Paton, C. Antipsychotic polypharmacy in schizophrenia: benefits and risks. *CNS Drugs* **25**, 383-99 (2011).
58. Foster, A. & King, J. Antipsychotic Polypharmacy. *Focus (Am Psychiatr Publ)* **18**, 375-385 (2020).
59. Roth, B.L., Sheffler, D.J. & Kroeze, W.K. Magic shotguns versus magic bullets: selectively non-selective drugs for mood disorders and schizophrenia. *Nat Rev Drug Discov* **3**, 353-9 (2004).
60. Nair, P.C., McKinnon, R.A., Miners, J.O. & Bastiampillai, T. Binding of clozapine to the GABA(B) receptor: clinical and structural insights. *Mol Psychiatry* **25**, 1910-1919 (2020).
61. Johnstone, T.B. et al. Allosteric modulation of related ligand-gated ion channels synergistically induces long-term potentiation in the hippocampus and enhances cognition. *The Journal of pharmacology and experimental therapeutics* **336**, 908-915 (2011).
62. Singhal, S.K., Zhang, L., Morales, M. & Oz, M. Antipsychotic clozapine inhibits the function of alpha7-nicotinic acetylcholine receptors. *Neuropharmacology* **52**, 387-94 (2007).
63. Simeone, X. et al. Molecular tools for GABAA receptors: High affinity ligands for  $\beta$ 1-containing subtypes. *Scientific Reports* **7**, 5674 (2017).
64. Simeone, X. et al. Defined concatenated  $\alpha$ 6 $\alpha$ 1 $\beta$ 3 $\gamma$ 2 GABA(A) receptor constructs reveal dual action of pyrazoloquinolinone allosteric modulators. *Bioorg Med Chem* **27**, 3167-3178 (2019).
65. Wongsamitkul, N. et al.  $\alpha$  subunits in GABA(A) receptors are dispensable for GABA and diazepam action. *Sci Rep* **7**, 15498 (2017).
66. Sali, A. & Blundell, T.L. Comparative protein modelling by satisfaction of spatial restraints. *J Mol Biol* **234**, 779-815 (1993).
67. Jones, G., Willett, P., Glen, R.C., Leach, A.R. & Taylor, R. Development and validation of a genetic algorithm for flexible docking. *J Mol Biol* **267**, 727-48 (1997).
68. Hawkins, P.C.D., Skillman, A.G., Warren, G.L., Ellingson, B.A. & Stahl, M.T. Conformer Generation with OMEGA: Algorithm and Validation Using High Quality Structures from the Protein Databank and Cambridge Structural Database. *Journal of Chemical Information and Modeling* **50**, 572-584 (2010).
69. Poli, G., Seidel, T. & Langer, T. Conformational Sampling of Small Molecules With iCon: Performance Assessment in Comparison With OMEGA. *Frontiers in Chemistry* **6**(2018).
70. Ashoor, A. et al. Effects of phenothiazine-class antipsychotics on the function of  $\alpha$ 7-nicotinic acetylcholine receptors. *European journal of pharmacology* **673**, 25-32 (2011).
71. Gotti, C., Riganti, L., Vailati, S. & Clementi, F. Brain neuronal nicotinic receptors as new targets for drug discovery. *Curr Pharm Des* **12**, 407-28 (2006).
72. Grinevich, V.P., Papke, R.L., Lippiello, P.M. & Bencherif, M. Atypical antipsychotics as noncompetitive inhibitors of alpha4beta2 and alpha7 neuronal nicotinic receptors. *Neuropharmacology* **57**, 183-191 (2009).
73. Weber, M.L. et al. Therapeutic doses of antidepressants are projected not to inhibit human  $\alpha$ 4 $\beta$ 2 nicotinic acetylcholine receptors. *Neuropharmacology* **72**, 88-95 (2013).

## Acknowledgements

The authors would like to thank Philip Schmiedhofer, Kevin John and Zarina Hogeckamp for their assistance with electrophysiological experiments. The authors K.B., F.K., T.S., A.G., T.L., M.E. gratefully acknowledge financial support from the European Community: The NeuroDeRisk project has received funding from the Innovative Medicines Initiative 2 Joint Undertaking under grant agreement No 821528. This Joint Undertaking receives support from the European Union's Horizon 2020 research and innovation programme and EFPIA. The authors K.B., F.D.V. and M.E. have received funding from the Austrian Science Fund in the MolTag doctoral program FWF W1232.

## **Author contributions**

K.B., M.W. and M.E. conceived the study. K.B. planned and supervised electrophysiological experiments. K.B., L.S., S.R., F.V. and F.Z. performed electrophysiological measurements and data analysis. F.K. performed structural analysis and computational docking. T.S., A.G. and T.L. performed pharmacophore analysis. K.B., and M.E. wrote the manuscript. K.B., F.K., F.V. and F.Z. prepared figures.

## **Additional information**

**Supplementary information** accompanies this paper.

**Competing interests:** The authors declare no competing interests.

**Declaration of transparency and scientific rigour:** This Declaration acknowledges that this paper adheres to the principles for transparent reporting and scientific rigour of preclinical research recommended by funding agencies, publishers and other organisations engaged with supporting research.